

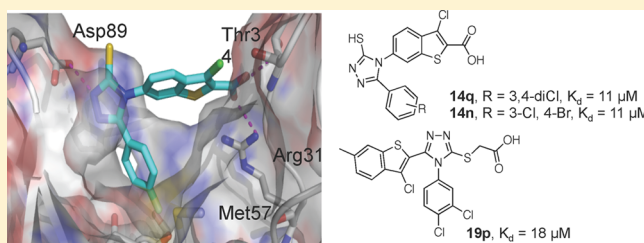
Discovery of Protein–Protein Interaction Inhibitors of Replication Protein A

James D. Patrone,^{†,||} J. Phillip Kennedy,^{†,||} Andreas O. Frank,^{†,⊥} Michael D. Feldkamp,[†] Bhavatarini Vangamudi,[†] Nicholas F. Pelz,[†] Olivia W. Rossanese,[†] Alex G. Waterson,^{‡,§} Walter J. Chazin,^{†,§} and Stephen W. Fesik^{*,†,‡,§}[†]Department of Biochemistry, [‡]Department of Pharmacology, Vanderbilt University School of Medicine, [§]Department of Chemistry, Vanderbilt University, Nashville, Tennessee 37232, United States

Supporting Information

ABSTRACT: Replication protein A (RPA) is a ssDNA binding protein that is essential for DNA replication and repair. The initiation of the DNA damage response by RPA is mediated by protein–protein interactions involving the N-terminal domain of the 70 kDa subunit with partner proteins. Inhibition of these interactions increases sensitivity toward DNA damage and replication stress and may therefore be a potential strategy for cancer drug discovery. Toward this end, we have discovered two lead series of compounds, derived from hits obtained from a fragment-based screen, that bind to RPA70N with low micromolar affinity and inhibit the binding of an ATRIP-derived peptide to RPA. These compounds may offer a promising starting point for the discovery of clinically useful RPA inhibitors.

KEYWORDS: Replication protein A, DNA damage, fragment-based discovery



Replication protein A (RPA) is a heterotrimeric single-stranded DNA (ssDNA) binding protein comprised of 70, 32, and 14 kDa subunits and is essential for eukaryotic DNA replication, damage response, and repair.^{1,2} RPA binds to ssDNA and protects it from degradation, while also functioning as a scaffold upon which DNA processing proteins assemble to initiate the response to DNA damage.^{3–8} ssDNA-binding is mediated by four oligonucleotide–oligosaccharide-fold (OB-fold) domains, which are present in the RPA70 and RPA32 subunits. The N-terminal OB-fold of the RPA70 subunit (RPA70N) does not bind with high affinity to ssDNA, but instead mediates binding to partner proteins involved in the DNA damage response pathway, such as p53, Rad9, ATRIP, and Mre11.^{5,6,9,10}

Disruption of the protein–protein interactions of RPA70N by mutation of either partner leads to decreased signaling through ATR and increased sensitivity to DNA damage and replication stress.^{5,11} Removal of the entire RPA protein through the use of siRNA, however, is cytotoxic to cells, as would be expected given the essential role of this protein in DNA metabolism.¹² We postulate that selective inhibition of only the RPA70N protein–protein interactions may offer a wider therapeutic window and a more targeted therapy. A small molecule that binds to the RPA70N protein-binding cleft would interfere with the interaction of RPA70N and its binding partners and thus prevent the initiation of the DNA damage response, while avoiding the deleterious effects of inhibiting ssDNA binding. Such a small molecule inhibitor of RPA70N may have therapeutic utility as a treatment for cancer in tumors

with high levels of replicative stress and may also potentiate the action of a number of current therapeutics. Thus far, only a limited number of RPA inhibitors have been reported. Turchi and colleagues have identified dihydropyrazole **1** from a screen of the National Cancer Institute (NCI) library and a ChemDiv library (Figure 1).^{12,13} In vitro, dihydropyrazole **1** binds to a DNA-binding domain of RPA and disrupts its interaction with DNA.^{12,13} Oakley and colleagues screened 1500 compounds from the NCI Diversity Set using an ELISA-type assay and have described fumaropimaric acid (**2**; Figure 1), which was shown to disrupt both RPA70N–Rad9 and RPA70N–p53 interactions.^{11,14}

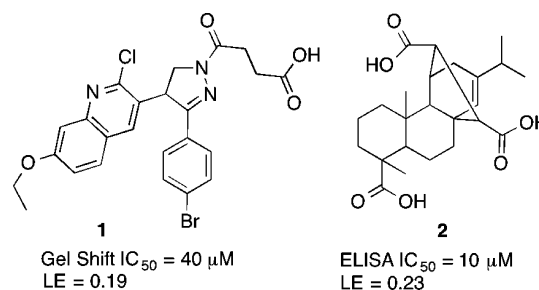


Figure 1. Compounds known to bind RPA.

Received: January 24, 2013

Accepted: May 1, 2013

Published: May 1, 2013

To identify an inhibitor of the protein–protein interactions of RPA70N, our 15,000-member fragment library was screened for binding to RPA70N using NMR. In this screen, over 150 fragment hits were identified with K_d values ranging from 600 μM to over 2000 μM and ligand efficiencies (LE) ranging from 0.15–0.32. Among the initial fragment hits, benzothiofene **3** ($K_d = 627 \mu\text{M}$, LE = 0.32) and tetrazole **4** ($K_d = 1850 \mu\text{M}$, LE = 0.32) were chosen for further optimization. In an attempt to produce rapid gains in binding affinity, we purchased more complex, commercially available compounds that combined features of these two fragment leads. As part of this effort, we identified the two lead molecules **5** and **6** with improved K_d values of 130 and 135 μM , respectively, but with reduced ligand efficiencies (Figure 2).

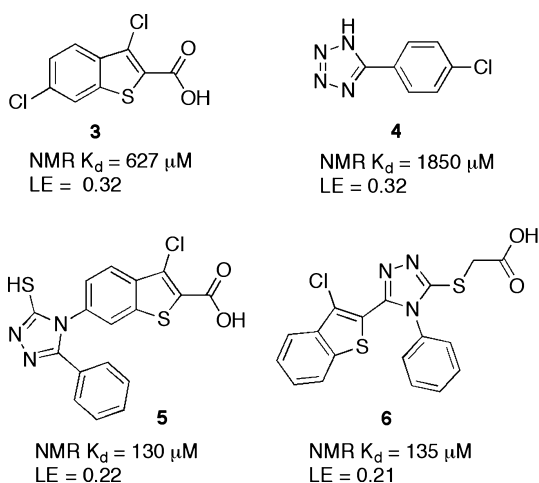
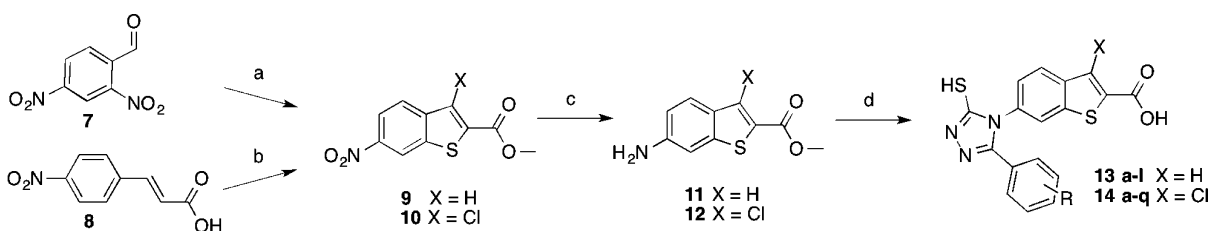


Figure 2. Initial fragment hits and lead series.

To explore the SAR of compound **5**, a synthetic strategy was developed that allowed variation of substituents on the phenyl ring at the 5-position of the triazole (Scheme 1). 2,4-Dinitrobenzaldehyde is condensed with methyl thioglycolate using microwave irradiation to form methyl 6-nitro-benzothiofene **9**.¹⁵ Alternatively, 4-nitrocinnamic acid is refluxed in the presence of thionyl chloride for 24 h.¹⁶ The addition of methanol affords methyl 3-chloro-6-nitro-benzothiofene carboxylate **10**.¹⁷ The nitro group on benzothiofenenes **9** and **10** is reduced using either 5% Pd/C or 5% Pt/C under a hydrogen atmosphere to yield anilines **11** and **12**, respectively. With the 6-position aniline on the benzothiofene in place, the 2-thio-5-phenyltriazole is formed in a three-step one-pot

Scheme 1. Synthesis of Analogues **13** and **14**^a

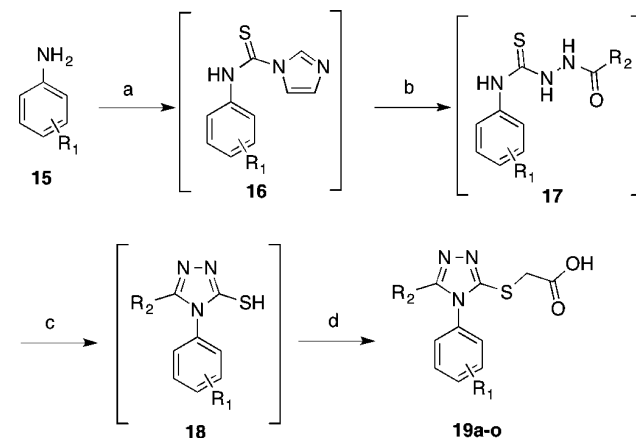


^aReagents and Conditions: (a) methyl thioglycolate, TEA, DMSO μW irradiation, 120 $^\circ\text{C}$, 30 min, 33%; (b) SOCl_2 , reflux then MeOH, 62%; (c) H_2 5% Pd/C or 5% Pt/C, 1:1 EtOAc/MeOH, 90–98%; (d) i. TCDI, DMF, μW irradiation, 60 $^\circ\text{C}$, 10 min, ii. R-Ar–CONHNH₂, μW irradiation, 60 $^\circ\text{C}$, 10 min, iii. 2M KOH, μW irradiation, 120 $^\circ\text{C}$, 30 min, 5–32%.

microwave cyclization sequence. Saponification of the ester affords final compounds **13a–l** and **14a–q**.¹⁸

The synthesis of compound **6** analogues was accomplished via a one-pot microwave cyclization and alkylation sequence (Scheme 2).¹⁸ The mixed thiourea **16** is formed from the

Scheme 2. Synthesis of Analogues **19a–o**^a



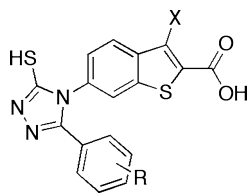
^aReagents and Conditions: (a) TCDI, DMF, μW irradiation, 85 $^\circ\text{C}$, 20 min; (b) $\text{R}_2\text{-CONHNH}_2$, μW irradiation, 75 $^\circ\text{C}$, 20 min; (c) 2M KOH, μW irradiation, 125 $^\circ\text{C}$, 20 min; (d) bromoacetic acid, 125 $^\circ\text{C}$, 20 min, 10–62%.

appropriate substituted aniline and 1',1'-thiocarbonyldiimidazole and the R_2 aromatic group is then installed via reaction of the mixed thiourea with a substituted hydrazide to form the semicarbazide intermediate **17**. The semicarbazide is cyclized under basic conditions to the thiotriazole intermediate **18**, which is then alkylated to give compounds **19a–o**.

Molecules were tested for their ability to bind RPA70N and displace a FITC-labeled ATRIP-derived peptide using a fluorescence polarization anisotropy (FPA) assay.¹⁹ Compounds that inhibit peptide binding result in a dose-dependent decrease in anisotropy, allowing for determination of IC_{50} values and calculation of K_d values. We have previously reported the use of this assay to measure a K_d of 18.3 μM for known compound **2**.^{11,19} Compound **1** did not inhibit the RPA70N-ATRIP interaction.

The first goal of the initial SAR was to evaluate the importance of the 3-position chloro substitution of the benzothiofene ring. On the basis of the poor binding ($K_d > 250 \mu\text{M}$) of compounds **13b–d** as compared to compounds **5** and **14a–c**, a chlorine at the 3-position appears important for binding (Table 1). Bromo- or chloro-substitutions on the 3- or 4-position of the phenyl ring also had a favorable effect on the

Table 1. SAR of Benzothiophene Lead Series



compd	X	R	K_d (μM) ^a
5	Cl	H	130
13a	H	H	>250
13b	H	2-Me	>250
13c	H	3-Me	>250
13d	H	4-Me	>250
13e	H	3-phenoxy	104
13f	H	3-Br	49
13g	H	4-Br	71
13h	H	4-Cl	78
13i	H	4-F	>250
13j	H	3-Cl, 4-Br	12
13k	H	3,5 diCl	35
13l	H	3,4 diCl	22
14a	Cl	2-Me	66
14b	Cl	3-Me	83
14c	Cl	4-Me	92
14d	Cl	3-phenoxy	63
14e	Cl	3-Br	58
14f	Cl	4-Br	42
14g	Cl	4-Cl	52
14h	Cl	4-F	47
14i	Cl	2-naphthyl ^b	43
14j	Cl	indole ^b	>250
14k	Cl	cyclohexyl ^b	25
14l	Cl	2-Br, 3-Me	48
14m	Cl	3-Me, 4-Br	31
14n	Cl	3-Cl, 4-Br	11 (10) ^c
14o	Cl	3-Br, 4-Cl	16
14p	Cl	3,5 di Cl	15
14q	Cl	3,4 di Cl	11 (17) ^c

^aAverage K_d values ($n = 2$) calculated from IC_{50} measured in FPA competition assay using Cheng–Prusoff equation. ^bThe entire phenyl ring is replaced by the indicated ring system. ^cAverage K_d values using RPA70NAB in FP assay.

binding affinity, as evidenced by compounds **13f–h**, with K_d values ranging from 49 to 78 μM . Similarly 3-chlorobenzothiophene analogues **14e–g** displayed even better affinities (K_d between 42 and 58 μM).

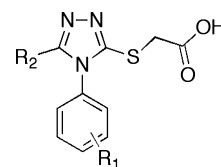
Additional substitutions on the phenyl ring were explored to further investigate the SAR. 3-Phenoxy analogues **13e** and **14d** were found to display only moderate binding affinities (K_d values of 104 and 63 μM , respectively) and sharply reduced ligand efficiencies (0.17 and 0.18 versus 0.22 for **5**). This was taken as evidence that the 3-phenoxy substitutions were likely too large for the binding pocket.

Replacement of the phenyl ring with a naphthyl moiety (**14i**) was tolerated and gave a K_d of 43 μM ; whereas replacement of the phenyl ring with an indole was unacceptable (**14j**; $K_d > 250$ μM). Interestingly, replacing the phenyl ring with a cyclohexyl ring (**14k**) produced one of our best compounds, with a K_d of 25 μM . On the basis of these results, we inferred that the molecules were likely binding into a lipophilic pocket of moderate size.

We next explored the effects of multiple substitutions of the 5-position phenyl ring of the triazole (Table 1), which was quite effective based on the binding affinities of compounds **14l–q** (K_d values 11–48 μM). A 3,4-disubstitution is generally preferred, and halogen substituents are favored over methyl groups. Indeed, the two compounds with the best binding affinities, **14n** and **14q** ($K_d = 11$ μM), both contain two halogen substituents in a 3,4-substituted pattern. Further evidence of this preferred substitution pattern is exemplified by **13j** ($K_d = 12$ μM), which retains good affinity even though it lacks the 3-chloro substitution on the benzothiophene ring.

On the basis of the SAR of triazoles **13** and **14**, the SAR of triazole **6** was initially explored using either a 3-chloro or 4-chloro substitution on the 1-position phenyl ring (Table 2).

Table 2. SAR of the Triazole Lead Series



compd	R ₁	R ₂	K_d (μM) ^a
6	H		135
19a	3-Cl	2-methylphenyl	>250
19b	3-Cl	2-chlorophenyl	>250
19c	3-Cl	2-bromophenyl	>250
19d	3-Cl	4-fluorophenyl	>250
19e	3-Cl	4-methoxyphenyl	>250
19f	3-Cl	2-naphthyl	122
19g	4-Cl	4-methoxyphenyl	>250
19h	4-Cl	4-fluorophenyl	>250
19i	3,4 diCl	4-methoxyphenyl	164
19j	3,4 diCl	4-hydroxyphenyl	233
19k	3,4 diCl	4-aminophenyl	109
19l	3,4 diCl	4-nitrophenyl	178
19m	3,4 diCl	2-naphthyl	47
19n	3,4 diCl		58
19o	3,4 diCl		46
19p	3,4 diCl		18

^aAverage K_d values ($n = 2$) calculated from IC_{50} measured in FPA competition assay using Cheng–Prusoff equation.

Replacement of the 5-position benzothiophene ring system with substituted phenyl rings was unsuccessful, as compounds **19a–e** and **19g–h** all possessed binding affinities greater than 250 μM . However, replacing the 5-position benzothiophene with a fused bicyclic aromatic system was better tolerated, as exemplified by **19f**. As observed in the benzothiophene series, employing a 3,4-dichloro substituted phenyl ring met with better results than mono halogenated compounds. Although analogues **19i–l**, with substituted phenyl rings in the 5-position of the triazole, exhibit K_d values below 250 μM , they still have reduced affinities relative to the lead molecule. The best

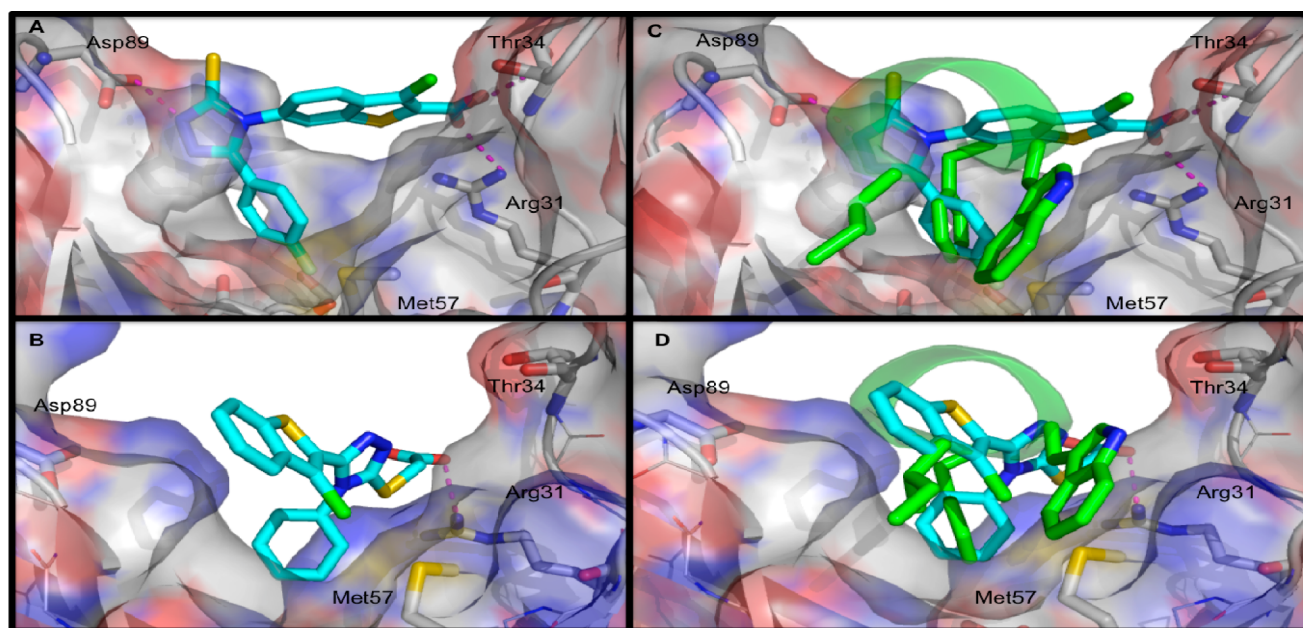


Figure 3. (A) Cocrystal structure of **14h** bound to RPA70N. (B) Cocrystal structure of **6** bound to RPA70N. (C) Cocrystal structure of **14h** bound to RPA70N overlaid with side chains of the RPA–p53 fusion protein. (D) Cocrystal structure of **6** bound to RPA70N overlaid with side chains of the RPA–p53 fusion protein.

compounds (**19m–p**) were obtained by utilizing the 3,4-dichloro substituted 1-position phenyl ring in combination with fused aromatic systems in the R_2 position. The best example was compound **19p** ($K_d = 18 \mu\text{M}$), with a 3-chloro-6-methylbenzothiophene in the R_2 position.

It has been proposed that the presence of additional RPA domains may influence the binding of compounds to RPA70N.¹⁴ We examined the ability of exemplar compounds **14n** and **14q** to bind to and displace the ATRIP peptide from RPA_{1–422}, which contains RPA70N and the adjacent tandem high affinity ssDNA-binding domains (RPA70NAB). No differences in binding affinity were observed for either compound in the presence of the additional domains ($K_d = 10$ and $17 \mu\text{M}$, respectively; Table 1).

To assess the domain specificity and functional selectivity of **14q** and **14n**, the compounds were analyzed for their ability to inhibit binding of full length heterotrimeric RPA to ssDNA using an electrophoresis mobility shift assay (EMSA). Neither **14q** nor **14n** showed evidence of disrupting RPA–ssDNA interactions at concentrations up to $100 \mu\text{M}$ (Supplementary Figure 1), indicating that these compounds are specific for inhibition of the RPA70N–ATRIP interaction.

Concurrent with the SAR efforts, we characterized the binding modes of the two different lead series using X-ray crystallography. Cocrystal structures of compounds **14h** and **6** bound to RPA70N (Figure 3) were obtained with several molecules in the asymmetric unit from compound soaked into crystals of E7R RPA70N.²⁰ This mutant protein crystallized in a different space group than the WT protein, allowing the binding cleft to be exposed and the structures of RPA70N/ligand complexes to be obtained.

Examination of the cocrystal structure of compound **14h** (Figure 3A) reveals several key features of the binding mode. The carboxylic acid in the 2-position of the benzothiophene is positioned in between Arg31 and Thr34 and forms an interaction with both residues. The 3-nitrogen of the triazole ring of **14h** makes a hydrogen bond with Asp89 on the back lip

of the binding pocket. This network of three hydrogen bonds is responsible for positioning the 3-chlorobenzothiophene core across the cleft of RPA70N so that it projects the phenyl ring at the 5-position of the triazole ring into a hydrophobic pocket that is created by Leu87 and Val93 on the side, the backbone of Ser54, Ser55, and Phe56 at the bottom and Met57 in the front. The small size and hydrophobic nature of the pocket makes clear the preference for small lipophilic substitutions on the phenyl ring that occupies this site.

As expected, triazole **6** binds to the basic cleft of RPA70N quite differently from benzothiophene **14h** (Figure 3B). However, the compound still makes several of the same key interactions. The thiomethyl linker allows the carboxylic acid on the 2-position of the triazole to extend far enough to form a hydrogen bond with Arg31, similar to the carboxylic acid of **14h**. In addition, the phenyl ring occupies the hydrophobic pocket formed by Ser54, Ser55, and Phe56 in a similar way to the phenyl ring of compound **14h**. This may explain the similar SAR preferences between the two series. While the triazole of compound **6** does not appear to make any polar contacts, the benzene ring of the 3-chlorobenzothiophene does engage in van der Waal interactions with Leu87, and the 3-chlorine may interact with the sulfur of Met57.

Overlaying these cocrystal structures onto the previously reported structure of a p53–RPA70N fusion protein reveals certain similarities in the key binding features (Figure 3C,D).⁶ The phenyl ring of Phe54 of the p53-derived peptide occupies the same hydrophobic pocket as the phenyl rings of both compounds **14h** and **6**. Compound **14h** does not appear to overlay well with any other residues of p53. However, the 3-chlorobenzothiophene of compound **6** fills a portion of the space that is occupied by the side chains of Ile50 and Trp53 in the p53 structure. The similarities in the binding modes of **6** and the p53 peptide suggest a possible strategy for improved compounds. One might envision placing a substitution on the 4-position of the benzothiophene of **14h** that incorporates the indole of the Trp53 of the p53 peptide (Figure 3C).

In conclusion, we have discovered two lead series derived from the hits obtained in a fragment-based screen. Compounds within these series represent the most potent inhibitors of the RPA70N–ATRIP protein–protein interaction reported to date, with no detectable inhibition of RPA–ssDNA interactions. To determine the molecular features that govern complex formation, we have obtained cocrystal structures of the two lead compounds, which help rationalize the SAR and provide structural information for the design of future inhibitors.

■ ASSOCIATED CONTENT

Supporting Information

Synthetic procedures and assay protocols. This material is available free of charge via the Internet at <http://pubs.acs.org>.

■ AUTHOR INFORMATION

Corresponding Author

*(S.W.F.) Tel: 615-322-6303. E-mail: stephen.fesik@vanderbilt.edu.

Present Address

[†]Novartis Institutes for BioMedical Research (NIBR), Global Discovery Chemistry, Emeryville, California 94608, United States.

Author Contributions

[‡]These authors contributed equally to this work.

Funding

Funding of this research was provided in part by NIH grants SDP1OD006933/8DP1CA174419 (NIH Director's Pioneer Award) to S.W.F., R01GM065484 to W.J.C., and ARRA stimulus grant (5RC2CA148375) to Lawrence J. Marnett. A.O.F. was supported by the Deutscher Akademischer Austausch Dienst postdoctoral fellowship and M.D.F. by the NIH NRSA postdoctoral fellowship.

Notes

The authors declare no competing financial interest.

■ ACKNOWLEDGMENTS

We would like to thank Dr. Dave Cortez for his intellectual contributions in the conception of this project and providing us with full length RPA.

■ REFERENCES

- (1) Wold, M. S. Replication protein A: A heterotrimeric, single-stranded DNA-binding protein required for eukaryotic DNA metabolism. *Annu. Rev. Biochem.* **1997**, *66*, 61–92.
- (2) Wold, M. S.; Kelly, T. Purification and characterization of replication protein-a, a cellular protein required for invitro replication of simian virus-40 DNA. *Proc. Natl. Acad. Sci. U.S.A.* **1988**, *85*, 2523–2527.
- (3) Iftode, C.; Borowiec, J. A. 5' → 3' Molecular polarity of human replication protein A (hRPA) binding to pseudo-origin DNA substrates. *Biochemistry* **2000**, *39* (39), 11970–11981.
- (4) Kim, C. S.; Paulus, B. F.; Wold, M. S. Interactions of human replication protein-a with oligonucleotides. *Biochemistry* **1994**, *33*, 14197–14206.
- (5) Xu, X.; Vaithiyalingam, S.; Glick, G. G.; Mordes, D. A.; Chazin, W. J.; Cortez, D. The basic cleft of RPA70N binds multiple checkpoint proteins, including RAD9, to regulate ATR signaling. *Mol. Cell. Biol.* **2008**, *28*, 7345–7353.
- (6) Bochkareva, E.; Kaustov, L.; Ayed, A.; Yi, G. S.; Lu, Y.; Pineda-Lucena, A.; Liao, J. C. C.; Okorokov, A. L.; Milner, J.; Arrowsmith, C. H.; Bochkarev, A. Single-stranded DNA mimicry in the p53 transactivation domain interaction with replication protein A. *Proc. Natl. Acad. Sci. U.S.A.* **2005**, *102*, 15412–15417.

- (7) Mer, G.; Bochkarev, A.; Gupta, R.; Bochkareva, E.; Frappier, L.; Ingles, C. J.; Edwards, A. M.; Chazin, W. J. Structural basis for the recognition of DNA repair proteins UNG2, XPA, and RAD52 by replication factor RPA. *Cell* **2000**, *103*, 449–456.

- (8) Brosh, R. M.; Orren, D. K.; Nehlin, J. O.; Ravn, P. H.; Kenny, M. K.; Machwe, A.; Bohr, V. A. Functional and physical interaction between WRN helicase and human replication protein A. *J. Biol. Chem.* **1999**, *274*, 18341–18350.

- (9) Ball, H. L.; Myers, J. S.; Cortez, D. ATRIP binding to replication protein A-single-stranded DNA promotes ATR-ATRIP localization but is dispensable for Chk1 phosphorylation. *Mol. Biol. Cell* **2005**, *16*, 2372–2381.

- (10) Braun, K. A.; Lao, Y.; He, Z. G.; Ingles, C. J.; Wold, M. S. Role of protein–protein interactions in the function of replication protein A (RPA): RPA modulates the activity of DNA polymerase α by multiple mechanisms. *Biochemistry* **1997**, *36*, 8443–8454.

- (11) Glanzer, J. G.; Liu, S. Q.; Oakley, G. G. Small molecule inhibitor of the RPA70 N-terminal protein interaction domain discovered using in silico and in vitro methods. *Bioorg. Med. Chem.* **2011**, *19*, 2589–2595.

- (12) Shuck, S. C.; Turchi, J. J. Targeted inhibition of replication protein A reveals cytotoxic activity, synergy with chemotherapeutic DNA-damaging agents, and insight into cellular function. *Cancer Res.* **2010**, *70*, 3189–3198.

- (13) Andrews, B. J.; Turchi, J. J. Development of a high-throughput screen for inhibitors of replication protein A and its role in nucleotide excision repair. *Mol. Cancer Ther.* **2004**, *3*, 385–391.

- (14) Glanzer, J. G.; Carnes, K. A.; Soto, P.; Liu, S.; Parkhurst, L. J.; Oakley, G. G. A small molecule directly inhibits the p53 transactivation domain from binding to replication protein A. *Nucleic Acids Res.* **2013**, *41*, 2047–59.

- (15) Fedi, V.; Altamura, M.; Catalioto, R. M.; Giannotti, D.; Giolitti, A.; Giuliani, S.; Guidi, A.; Harmat, N. J. S.; Lecci, A.; Meini, S.; Nannicini, R.; Pasqui, F.; Tramontana, M.; Triolo, A.; Maggi, C. A. Discovery of a new series of potent and selective linear tachykinin NK2 receptor antagonists. *J. Med. Chem.* **2007**, *50*, 4793–4807.

- (16) Castle, S. L.; Buckhaults, P. J.; Baldwin, L. J.; Mckenney, J. D.; Castle, R. N. The synthesis of monomethoxy[1]benzo-thieno[2,3-C]quinolines. *J. Heterocycl. Chem.* **1987**, *24*, 1103–1108.

- (17) Isloor, A. M.; Kalluraya, B.; Pai, K. S. Synthesis, characterization and biological activities of some new benzo[b]thiophene derivatives. *Eur. J. Med. Chem.* **2010**, *45*, 825–830.

- (18) Deprez-Poulain, R. F.; Charton, J.; Leroux, V.; Deprez, B. P. Convenient synthesis of 4H-1,2,4-triazole-3-thiols using di-2-pyridylthionocarbonate. *Tetrahedron Lett.* **2007**, *48*, 8157–8162.

- (19) Souza-Fagundes, E. M.; Frank, A. O.; Feldkamp, M. D.; Dorset, D. C.; Chazin, W. J.; Rossanese, O. W.; Olejniczak, E. T.; Fesik, S. W. A high-throughput fluorescence polarization anisotropy assay for the 70N domain of replication protein A. *Anal. Biochem.* **2012**, *421*, 742–749.

- (20) Feldkamp, M. D.; Frank, A. O.; Vangamudi, B.; Fesik, S. W.; Chazin, W. J. Surface engineering to optimize structural analysis of ligand binding to the N-terminal domain of the RPA70 subunit. *Biochemistry*, submitted for publication.